How to handle glacier area change in geodetic mass balance

Caitlyn Florentine[1], Louis Sass[2], Christopher McNeil[2] , Emily Baker[2] and Shad O'Neel[3]

[1]U.S. Geological Survey, Northern Rocky Mountain Science Center, West Glacier, MT, USA; [2]U.S. Geological Survey, Alaska Science Center, Anchorage, AK, USA and [3]U.S. Army Corps of Engineers, Cold Regions Research and Engineering Laboratory, Hanover, NH, USA

Abstract

Innovations in geodesy enable widespread analysis of glacier surface elevation change and geodetic mass balance. However, coincident glacier area data are less widely available, causing inconsistent handling of glacier area change. Here we quantify the bias introduced into meters water equivalent (m w.e.) specific geodetic mass balance results when using a fixed, maximum glacier area, and illustrate the bias for five North American glaciers. Sites span latitudes from the northern U.S. Rocky Mountains (48°N) to the Central Alaska Range (63°N) between 1948 and 2021. Results show that fixed (maximum) area treatment subdues the m w.e. mass change signal, underestimating mass balance by up to 19% in our test cases. This bias scales with relative glacier area change and the mass balance magnitude. Thus, the bias for specific geodetic mass balances will be most pronounced across rapidly deglaciating regions. Our analysis underscores the need for temporally resolved glacier area in geodetic mass balance studies.

1. Introduction

Geodetic glacier mass balance approaches have become increasingly common due to advances in global glacier inventories (Pfeffer and others, 2014) and elevation data availability (Farr and others, 2007; European Space Agency, 2010, 2022; Porter and others, 2018; Wessel and others, 2018; Neumann and others, 2019; U.S. ASTER Science Team, 2022). Hydrologically meaningful glacier mass balance estimates require accounting for the changing glacier area. Previous research elucidates the differences between glaciological and modeling techniques that use a fixed (reference) vs evolving (conventional) glacier surface (Elsberg and others, 2001; Cogley and others, 2011; Huss and others, 2012). However, the evaluation of fixed vs time-varying glacier area treatment for geodetic methods is relatively underdeveloped.

Reanalysis studies have emphasized the importance of consistent area treatment between geodetic and glaciological balances (e.g. Zemp and others, 2013). Geodetic glacier mass balances account for the changing glacier area where such glacier area data are available (Fischer and others, 2015; Magnússon and others, 2016; Dussaillant and others, 2018; Florentine and others, 2018; Belart and others, 2019; Falaschi and others, 2019; Zemp and others, 2019; Kapitsa and others, 2020; Hugonnet and others, 2021; Mukherjee and others, 2022). However, in many standalone remote sensing studies, the specific geodetic glacier mass balances reflect a fixed glacier area (Brun and others, 2017; Menounos and others, 2018; Dussaillant and others, 2019; Shean and others, 2020; Jakob and others, 2021). This is due to the dearth of time-varying glacier area data that correspond to the timing of elevation data acquisition. Whereas photogrammetry routines have automated the generation of DEMs from stereoscopic aerial or satellite imagery (Shean and others, 2016; Knuth and others, 2023) the automatic generation of glacier outlines has advanced (Roberts-Pierel and others, 2022) but is not as widespread or reliable.

Previous studies concluded that fixed area treatment had minor effects on regional mass balance rates (1–3%), but considerable effects (10%) for fast-retreating glaciers (Fischer and others, 2015; Falaschi and others, 2017). Studies in the European Alps have shown that fixed area treatment can underestimate glacier mass change rates by 14% (Sommer and others, 2020). Fixed area treatment is thus a potentially impactful source of systematic bias on specific geodetic mass balance where glacier area is rapidly changing.

Geodetic glacier mass balance uncertainties rarely if ever formally incorporate the effects of fixed area treatment. Uncertainties account for random error associated with the mass to density conversion, elevation error and/or error in temporally discrete glacier area data associated with glacier margin delineation (Brun and others, 2017; Florentine and others, 2018; O'Neel and others, 2019; McNeil and others, 2020; Shean and others, 2020; Mukherjee and others, 2022). Occasionally, geodetic mass balance error budgets account for other sources of systematic uncertainty associated with elevation change including imperfect sensor geometry and coregistration, but not glacier area change (Brun and others, 2017; Menounos and others, 2018; McNeil and others, 2020).

Here we assess the bias introduced by treating glacier area as fixed at the maximum during specific geodetic glacier mass balance calculation. First, we define the systematic bias introduced by the fixed (maximum) area treatment in general terms. Then, we quantify the bias

for geodetic mass balance results for U.S. Geological Survey Benchmark Glaciers, which employ 36 digital elevation models (DEMs) and coincident glacier area data dating from 1948 to 2021 (McNeil and others, 2019).

2. Methods

2.1. Time-varying glacier area treatment

Geodetic mass balance accounting for real-world changes in glacier area (Zemp and others, 2019) is given by:

$$B = \frac{\Delta V}{\bar{S}} \frac{\bar{\rho}}{\rho_w} \frac{1}{\Delta t} \tag{1}$$

here ΔV is the glacier volume change, $\bar{S}$ is the average glacier area over the period of measurement, $\bar{\rho}$ is the average material density, ρ_w is the density of water (1000 kg m^{-3}), and Δt is the measurement period. The $\bar{\rho}/\rho_w$ term constitutes a density conversion factor, which is routinely assigned as 0.850 when the time interval is longer than five years and the glacier mass balance rate exceeds 0.2 m water equivalent per year (m w.e. a^{-1}) (Huss, 2013). The geodetic mass balance B is intercomparable with conventional glaciological balances and can be used to calibrate glaciological time series. The time-varying area treatment in Eqn (1) reflects the real-world, changing glacier area.

2.2. Fixed glacier area treatment

Time-varying glacier area data are not always available. Therefore, in many standalone remote sensing studies, glacier area is treated as fixed. This fixed area is commonly assumed to be the maximum glacier area, S_{max}, giving:

$$B_{fixed} = \frac{\Delta V}{S_{max}} \frac{\bar{\rho}}{\rho_w} \frac{1}{\Delta t} \tag{2}$$

Equation (2) estimates the overall glacier mass change associated with changes in surface elevation, averaged across the fixed maximum glacier area. Relative to Eqn (1), such solutions poorly represent real-world physical processes, including area change, and are difficult to compare with glaciological balances that account for changing glacier area. It does not enable intercomparison across glaciers experiencing varying rates of area change.

2.3. Systematic bias and relative area change

The bias (δ, m w.e. a^{-1}) introduced by using a fixed, maximum glacier area is:

$$\delta = B - B_{fixed} \tag{3}$$

The ΔV, $\bar{\rho}$, ρ_w and Δt are identical for B and B_{fixed}, therefore Eqn (2) can be expressed in terms of the geodetic balance, and the bias is:

$$\delta = B - \frac{\bar{S}}{S_{max}} B \tag{4}$$

For inter-method comparison, the average glacier area ($\bar{S}$) is calculated from the same area time series used in the glaciological mass balances. If the rate of area change is linear, then $\bar{S}$ can be approximated as the average of the maximum and minimum glacier areas ($(S_{max} + S_{min})/2$). Note that area change is not linear in cases of glacier surging or other irregular patterns of glacier area

change during the geodetic measurement interval. Substituting into Eqn (4) yields:

$$\delta = B \left(1 - \frac{(S_{max} + S_{min})}{2S_{max}} \right) = B \left(1 - \frac{S_{max}}{2S_{max}} - \frac{S_{min}}{2S_{max}} \right)$$
$$= \frac{1}{2} B \left(1 - \frac{S_{min}}{S_{max}} \right) \tag{5}$$

This defines the bias in terms of relative glacier area change ($\Delta S/S_{max}$) = $((S_{max} - S_{min})/S_{max})$ = $1 - (S_{min}/S_{max})$. Hence the fixed, maximum area bias is predictable as a function of the relative glacier area change and glacier mass balance:

$$\delta = \frac{1}{2} B \left(\frac{\Delta S}{S_{max}} \right) \tag{6}$$

2.4. Application to benchmark glaciers

Next, we illustrate and quantify the bias introduced by the fixed, maximum area treatment using applied cases from the tested geodetic mass balance time series. We employ geodetic data collected on the U.S. Geological Survey Benchmark Glaciers. These five glaciers span the climate zones that support glacierized mountains in Alaska and the contiguous U.S. including midlatitude continental (Sperry Glacier), midlatitude maritime (South Cascade Glacier), high-latitude maritime (Wolverine and Lemon Creek Glaciers), and high-latitude continental (Gulkana Glacier). The U.S. Geological Survey started an ongoing program of glaciological research in 1957 for the International Geophysical Year. South Cascade, Wolverine and Gulkana Glaciers are World Glacier Monitoring Service reference glaciers with more than 30 years of uninterrupted seasonal glaciological mass balance measurements.

Glacier area is known at multiple times throughout the observational period. The rate of glacier area change from each start date to end date in this tested dataset is approximated as linear. The mean difference between average areas computed using multiple glacier area timestamps, i.e. every available glacier area (S_e, Table 1) and the $\bar{S} = ((S_{max} + S_{min})/2)$ approximation is 2.01% and the std dev. is 2.38% (Table 1). In the benchmark glacier dataset, the maximum area corresponds to the start of the geodetic interval, and the minimum area corresponds to the end.

In this study, the fixed area bias is calculated for every geodetic time interval (e.g. 1967 to 2016, 1974 to 2016, etc.). The time interval is defined by the acquisition date and the date of the reference DEM used for coregistration. We used DEMs and glacier outlines covering the benchmark glaciers between 1948 and 2021 derived from aerial and satellite stereo image pairs ($n = 33$), historic topographic maps ($n = 2$), and Shuttle Radar Topography Mission data ($n = 1$) (McNeil and others, 2019). Glacier area data and DEMs were derived from the same source imagery, therefore glacier area dates coincide with elevation data timing. Geodetic mass balance results reflect Eqn (1) and details outlined in O'Neel and others (2019), except that here DEM alignment was executed using automated coregistration (Shean and others, 2016), geodetic intervals are all longer than five years, and geodetic balance rates exceed 0.2 m w.e. a^{-1}.

Glacier volume change (ΔV) and geodetic mass balance (B) results presented in this study were executed using DEM pair differencing. Universal coregistration (Nuth and Kääb, 2011) was used to align DEMs by minimizing offsets in snow-free, off-glacier, stable bedrock terrain. Voids in the DEMs were filled using a regression between elevation and surface elevation change (McNabb and others, 2019). DEM dates are listed in Table 1 and were selected to correspond with the timing of annual glacier

Table 1. Geodetic results. S_{max} is the maximum and S_{min} is the minimum glacier area between the start and end dates of the geodetic measurement period. $\bar{S}_e$ is the average area computed using every available area, and $\bar{S}$ is the average area assuming linear area change computed using only the maximum and minimum. Geodetic mass balance (B) and interval length (dt) are listed.

Glacier	Start date	End date	dt Year	S_{max} km²	S_{min} km²	$\bar{S}$ km²	$\bar{S}_e$ km²	$\bar{S} - \bar{S}_e$ km²	B m w.e. a⁻¹
Gulkana	8/31/1967	8/30/2016	49	18.6	16.0	17.3	17.3	0.02	−0.59 ± 0.13
Gulkana	09/04/1974	8/30/2016	42	18.4	16.0	17.2	17.1	0.08	−0.60 ± 0.10
Gulkana	08/25/1979	8/30/2016	37	18.1	16.0	17.1	16.9	0.17	−0.60 ± 0.09
Gulkana	07/11/1993	8/30/2016	23	18.0	16.0	17.0	16.6	0.33	−0.80 ± 0.22
Gulkana	08/08/2005	8/30/2016	11	16.9	16.0	16.4	16.3	0.13	−0.72 ± 0.21
Gulkana	08/11/2007	8/30/2016	9	16.9	16.0	16.4	16.1	0.31	−0.70 ± 0.10
Gulkana	8/30/2016	09/19/2021	5	16.0	15.5	15.7	15.5	0.25	−0.69 ± 0.16
Wolverine	08/07/1950	09/12/2018	68	17.5	15.6	16.6	16.5	0.04	−0.30 ± 0.22
Wolverine	08/25/1969	09/12/2018	49	17.1	15.6	16.4	16.4	−0.03	−0.35 ± 0.08
Wolverine	09/13/1972	09/12/2018	46	17.0	15.6	16.3	16.3	0.04	−0.41 ± 0.07
Wolverine	08/03/1979	09/12/2018	39	17.0	15.6	16.3	16.2	0.14	−0.47 ± 0.11
Wolverine	09/27/1995	09/12/2018	23	16.8	15.6	16.2	16.	0.20	−0.61 ± 0.10
Wolverine	08/08/2006	09/12/2018	12	16.4	15.6	16.0	15.8	0.18	−0.72 ± 0.58
Lemon Creek	08/13/1948	10/01/2018	70	12.8	9.7	11.2	11.2	0.1	−0.69 ± 0.22
Lemon Creek	09/18/1957	10/01/2018	61	12.4	9.7	11.0	11.0	0.1	−0.71 ± 0.07
Lemon Creek	08/30/1974	10/01/2018	44	12.1	9.7	10.9	10.8	0.1	−0.93 ± 0.10
Lemon Creek	08/11/1979	10/01/2018	39	12.1	9.7	10.9	10.6	0.3	−1.05 ± 0.28
Lemon Creek	08/28/1989	10/01/2018	29	11.7	9.7	10.7	10.4	0.3	−1.12 ± 0.18
Lemon Creek	02/11/2000	10/01/2018	18	10.7	9.7	10.2	10.1	0.1	−1.35 ± 0.24
Lemon Creek	09/04/2013	10/01/2018	5	10.4	9.7	10.0	9.9	0.1	−2.46 ± 0.29
South Cascade	08/13/1958	10/14/2015	57	2.9	1.8	2.38	2.31	0.06	−0.73 ± 0.10
South Cascade	09/29/1970	10/14/2015	45	2.7	1.8	2.28	2.24	0.04	−0.72 ± 0.05
South Cascade	10/06/1979	10/14/2015	36	2.6	1.8	2.23	2.18	0.05	−0.87 ± 0.07
South Cascade	09/05/1986	10/14/2015	29	2.6	1.8	2.20	2.12	0.08	−0.90 ± 0.10
South Cascade	10/06/1992	10/14/2015	23	2.3	1.8	2.06	2.04	0.02	−0.84 ± 0.07
South Cascade	09/20/2001	10/14/2015	14	2.2	1.8	1.99	1.99	0.00	−0.93 ± 0.09
South Cascade	09/26/2004	10/14/2015	11	2.1	1.8	1.98	1.95	0.03	−0.84 ± 0.13
South Cascade	10/01/2008	10/14/2015	7	2.0	1.8	1.93	1.89	0.04	−0.77 ± 0.07
South Cascade	10/14/2015	08/13/2021	6	1.8	1.8	1.81	1.80	0.01	−0.79 ± 0.09
Sperry	09/01/1950	09/07/2014	64	1.3	0.8	1.1	1.01	0.1	−0.24 ± 0.03
Sperry	09/08/1960	09/07/2014	54	1.2	0.8	1.0	0.94	0.09	−0.26 ± 0.04

mass minimum at the end of the summer melt season. Geodetic glacier mass balance uncertainties account for error on the elevation change signal and uncertainty in the volume to mass conversion associated with material density assumptions (Florentine and others, 2018; O'Neel and others, 2019).
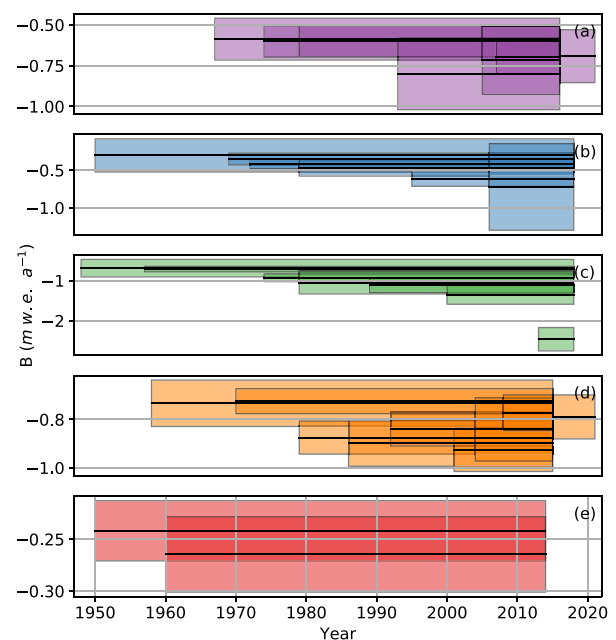
Fixed maximum glacier area handling subdues the m w.e. a⁻¹ signal, but to varying degrees, in proportion to the geodetic results particular to each measurement interval. The biases tested here ranged from 0.01 to 0.19 as a fraction of the mass balance (Fig. 3). The fixed area treatment therefore underestimates mass balance by 1 to 19% for these test cases.

3. Results

Benchmark glacier geodetic balances range from −0.24 to −2.46 m w.e. a⁻¹, relative area changes range from 1 to 38%, and the biases range from −0.01 to −0.14 m w.e. a⁻¹ (Figs 1, 2, Table 1). The largest bias was found for South Cascade Glacier in the 1958 to 2015 period, which had a geodetic balance of −0.73 m w.e. a⁻¹ and relative area change of 38%.

Big relative area change for the benchmark glaciers generally corresponds to larger bias (Fig. 2). Similarly, small relative area change for benchmark glaciers can correspond to smaller bias, but not necessarily, because the bias is driven by both the relative area change and the magnitude of the geodetic mass balance (Eqn (6)). For example, the bias for Wolverine Glacier is 0.016 m w.e. a⁻¹ for both the 2006 to 2018 and 1950 to 2018 intervals, though the relative area change was 4 and 11% respectively. The smaller relative area change in the 2006 to 2018 interval is offset by larger geodetic mass balance (−0.72 m w.e. a⁻¹), and the larger relative area change in the 1950–2018 interval is offset by smaller geodetic mass balance (−0.30 m w.e. a⁻¹).

Figure 2 illustrates this concept, showing, for example, that the −0.1 m w.e. a⁻¹ fixed (maximum) area bias is possible for a range of relative area change and mass balance scenarios. Hence bias is not necessarily biggest for the fastest mass change rates or most relative area change. Rather the combination of fast retreating, fast thinning glaciers show the greatest bias between area treatments.
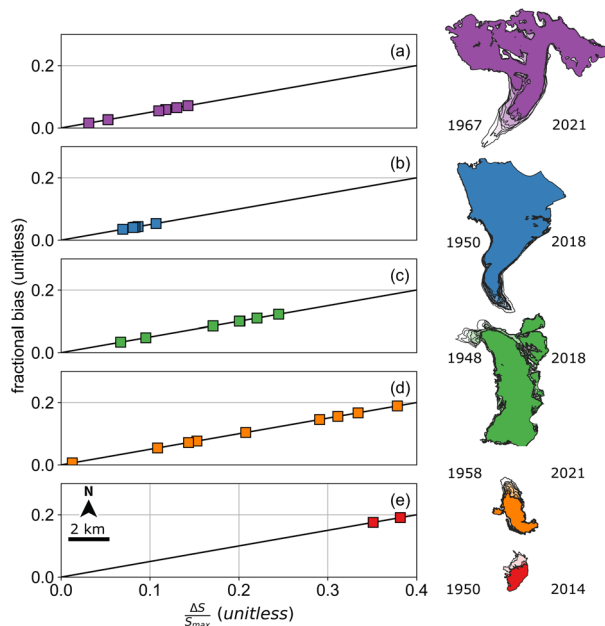

Figure 1. Geodetic mass balance (black) with error (color) for (a) Gulkana, (b) Wolverine, (c) Lemon Creek, (d) South Cascade and (e) Sperry Glaciers.
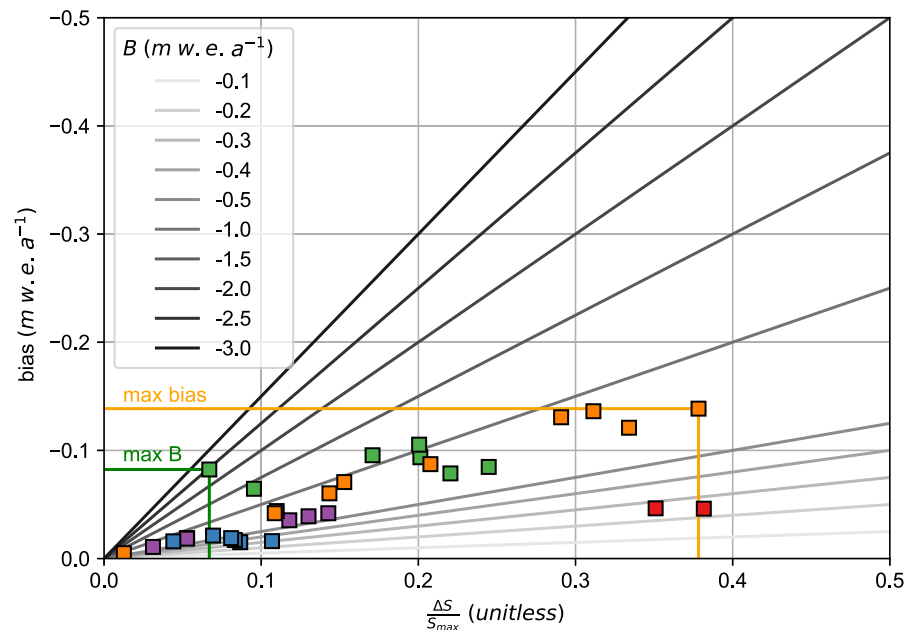
Figure 2. Bias introduced by the fixed, maximum area treatment, expressed as a function of relative area change. Hypothetical balances *(B)* are shown by solid grayscale lines. Results for this study are shown by colored squares for Gulkana (purple), Wolverine (blue), Lemon Creek (green), South Cascade (orange) and Sperry (red) Glaciers. Orange and green lines show that the maximum bias does not correspond to the maximum balance.

Figure 3. The fixed (maximum) area treatment underestimates mass balance by a fractional bias that is half the relative area change. The x-axis shows the relative area change $(\Delta S/S_{max})$ and the y-axis shows $(1/2)(\Delta S/S_{max})$ which, as shown by Eqn (6), is equivalent to the bias over the specific geodetic mass balance, i.e. (δ/B) the fractional bias. Results for this study are shown by colored squares for (a) Gulkana, (b) Wolverine, (c) Lemon Creek, (d) South Cascade and (e) Sperry Glaciers. Glacier area change is shown by glacier maps. North arrow and scale bar shown on inset of (e). First (left) and last (right) dates of the measurement period are indicated.

Our results illustrate how the fixed (maximum) area handling bias is predictable when glacier area dates correspond to DEM dates and the relative area change over the geodetic measurement interval is known. Figure 3 shows the linear relationship between relative area change and relative bias, where area change is expressed relative to the maximum area $(\Delta S/S_{max})$ and bias is expressed relative to the specific geodetic mass balance (δ/B). This fractional bias is one half the relative area change, as shown by Eqn (6) $((\delta/B) = (1/2)(\Delta S/S_{max}))$. Thus 38% relative area change results in 19% fixed area treatment bias.

4. Discussion

4.1. Toward clarity in area handling

Previous researchers have explored the effects of using a single glacier area on select geodetic mass balance results, but have not described the area handling bias beyond discrete sensitivity tests (Fischer and others, 2015; Brun and others, 2017; Falaschi and others, 2017; Dussaillant and others, 2019; Sommer and others, 2020). Here we described the fixed-area bias in general terms and present a method to correct the bias that can be applied to any glacier study where the maximum and minimum glacier areas during the measurement period are known, and the rate of glacier area change can be approximated as linear. These conditions are likely not met in glacier surge situations or where there is mismatch between the glacier area date and the elevation change measurement.

Furthermore, the bias definition asserts that the fixed area is the maximum, but the known area may not always represent the maximum area. Not only will the bias not be predictable when the true maximum glacier area is not used, the glacier volume change will have unknown error. The use of a smaller area crops the total glacier, consequently underestimating the total volume change. Depending on the rate of change within the omitted area this could lead to either an underestimate or an overestimate of average thinning rates. Hence the error that is introduced by using fixed glacier area that does not align with the maximum has an unknown effect.

Global studies of glacier change approach glacier area assuming a linear change through time, calibrated to available data that capture relative glacier area change for glacierized regions worldwide (Zemp and others, 2019; Hugonnet and others, 2021). These studies use the available estimates presented in IPCC AR5 (chapter 4, figure 4.10, table 4.SM.1) (Vaughan and others, 2013). However, these data reflect variable dates and measurement intervals, and do not encompass the comprehensive population of global glaciers. It is assumed that the available dataset on glacier relative area change is spatially and temporally representative. Future studies could explore the impact of these assumptions by comparing this baseline dataset against regionally complete inventories of glacier area change.

4.2. Need for temporally varying area

The fixed area treatment yields results that are biased compared with glaciological balances that incorporate glacier hypsometry

and surface area change over time (Sommer and others, 2020). Averaging the glacier mass change signal across the average glacier area yields results that are comparable to conventional balances (Elsberg and others, 2001; Cogley and others, 2011; Huss and others, 2012). In contrast, we show that averaging the glacier mass change signal across the fixed, maximum glacier area without resolving the time-evolving glacier footprint underestimates the mass change signal. Our results therefore underscore the importance of precise glacier area time series for calculating geodetic mass balance.

Temporal bias between the acquisition date of the glacier outline and the elevation change observations will yield unpredictable bias. Fixing the glacier area to an outline that does not represent the maximum glacier extent biases the glacier height change, volume change and geodetic mass balance. The Randolph Glacier Inventory (RGI; Pfeffer and others, 2014) provides a globally complete inventory of glacier area for one snapshot in time. Comparing benchmark glacier area data to the RGI suggest that pairing historic elevation data with RGI glacier area dates can alter geodetic mass balance results in variable ways (Table 2). The RGI 6.0 time stamps are up to 57 years past and 59 years before our geodetic measurement dates. The RGI 6.0 areas are up to 26% smaller or 63% bigger than our geodetic observations of glacier area for each measurement date (Table 2) due to the temporal mismatch between source imagery used to delineate glacier outlines. Additional sources of uncertainty affect glacier outlines due to inadvertent inclusion of

seasonal snow or differences in manual tracing (Paul and others, 2013).

Using the RGI area with the benchmark glacier DEM data in this study would introduce variable and unpredictable bias to the specific geodetic mass balance. To explore this effect, we computed the average height change across the RGI area and compared it to the average height change across the glacier area at each time step. We did not interpolate the DEM or convert glacier height change to mass change, to consider strictly the raw elevation differences between co-registered DEM data. These differences ranged from −10 to +35%, with median value of +2% and std dev. of 11%. This exercise illustrates the variable and nontrivial error introduced by using glacier areas that are not necessarily contemporaneous with the DEM acquisition date.

Using the RGI 6.0 glacier area footprint in our study would either sample bare ground and thereby dampen the volume change signal or exclude glacier ice and thereby yield results for some unknown portion of the glacier mass change. Including nonglacierized terrain may incorporate elevation change signals caused by changing proglacial area, e.g. outlet stream meandering, moraine erosion and hillslope instability, and attribute them inaccurately to glacier change. Similarly, excluding glacierized terrain misses some portion of the glacier elevation change signal. Depending on how fast the excluded portion of glacier is thinning (or thickening) compared to the measured portion of the glacier this can result in either larger or smaller estimates of specific geodetic mass balance.

4.3. Implications for calibrating glaciological measurements

We find that calibrating glaciological measurements with specific geodetic balances that have not handled changing glacier area biases the cumulative mass balance trend. Glaciological data capture interannual variability in mass balance, but do not reliably capture the mass balance trend, and therefore cannot independently validate the cumulative glacier mass balance (Zemp and others, 2013). Therefore, geodetic mass balance results are used to calibrate the glaciological balances, to reduce systematic bias caused by stake placement (O'Neel and others, 2019). For example, geodetic calibration executed in the O'Neel and others (2019) mass balance reanalysis of the benchmark glaciers showed that uncalibrated glaciological measurements at Wolverine Glacier for the 1980 to 2006 interval yield a positive trend in mass balance and net mass gain, which is inconsistent with observations of glacier retreat during this interval. The geodetic results yield a negative trend, indicating that the glaciological data underestimate ablation or overestimate accumulation. The glaciological data required nearly one meter per year (−0.98 m w.e. a^{-1}) calibration.

The benchmark glacier uncalibrated, conventional glaciological measurements reflect a time-varying glacier surface, wherein glacier hypsometry is updated annually and the m w.e. a^{-1} time series corresponds to smaller and smaller glacier areas over the time interval. In contrast, geodetic balances computed using the fixed (maximum) area treatment do not evolve the glacier area. This dampens the specific geodetic mass balance signal. Thus, even though the fixed (maximum) area treatment on the geodetic balance is biased, it reduces the mismatch with the positive uncalibrated glaciological trend. Indeed, fixed (maximum) area treatment on specific geodetic balances reduces the mismatch for all benchmark glaciers and every time interval ($n = 31$). The mismatch with uncalibrated glaciological data using fixed (maximum) area treatment on the geodetic mass balance is −0.51 m w.e. a^{-1}, whereas the mismatch using the time-varying area treatment is −0.55 m w.e. a^{-1}.

Correcting the area handling bias does not necessarily close the gap between uncalibrated, conventional glaciological

Table 2. Glacier areas and geodetic measurement dates used in this study (S, t) compared to RGI 6.0 glacier areas and dates (S_{RGI}, t_{RGI}). Percent difference between areas (S and S_{RGI}) is reported in the last column. Negative indicates that the RGI 6.0 area is smaller than the observed area.

	t Year	t_{RGI} Year	$t_{RGI} - t$ Year	S km^2	S_{RGI} km^2	$S_{RGI} - S$ km^2	$\frac{S_{RGI} - S}{S}$ %
Gulkana	1967	2006	39	18.6	17.6	−1.1	−5.9
Gulkana	1974	2006	32	18.4	17.6	−0.8	−4.3
Gulkana	1979	2006	27	18.1	17.6	−0.5	−2.8
Gulkana	1993	2006	13	18.0	17.6	−0.4	−2.2
Gulkana	2005	2006	1	16.9	17.6	0.7	4.1
Gulkana	2007	2006	−1	16.9	17.6	0.7	4.1
Gulkana	2016	2006	−10	16.0	17.6	1.6	10
Gulkana	2021	2006	−15	15.5	17.6	2.1	14
Wolverine	1950	2009	59	17.5	16.8	−0.7	−4.0
Wolverine	1969	2009	40	17.1	16.8	−0.3	−1.8
Wolverine	1972	2009	37	17.0	16.8	−0.2	−1.2
Wolverine	1979	2009	30	17.0	16.8	−0.2	−1.2
Wolverine	1995	2009	14	16.8	16.8	0.0	0.0
Wolverine	2006	2009	3	16.4	16.8	0.6	3.1
Wolverine	2018	2009	−9	15.6	16.8	1.2	7.7
Lemon Creek	1948	2005	57	12.8	9.5	−3.3	−26
Lemon Creek	1957	2005	48	12.4	9.5	−2.9	−23
Lemon Creek	1974	2005	31	12.1	9.5	−2.6	−21
Lemon Creek	1979	2005	26	12.1	9.5	−2.6	−21
Lemon Creek	1989	2005	16	11.7	9.5	−2.2	−19
Lemon Creek	2000	2005	5	10.7	9.5	−1.2	−11
Lemon Creek	2013	2005	−8	10.4	9.5	−0.9	−9
Lemon Creek	2018	2005	−13	9.7	9.5	−0.2	−2
South Cascade	1958	1958	0	2.9	2.9	0	0
South Cascade	1970	1958	−12	2.7	2.9	0.2	7.4
South Cascade	1979	1958	−21	2.6	2.9	0.3	12
South Cascade	1986	1958	−28	2.6	2.9	0.3	12
South Cascade	1992	1958	−34	2.3	2.9	0.6	26
South Cascade	2001	1958	−43	2.2	2.9	0.7	32
South Cascade	2004	1958	−46	2.1	2.9	0.8	38
South Cascade	2008	1958	−50	2.0	2.9	0.9	45
South Cascade	2015	1958	−57	1.8	2.9	1.1	61
South Cascade	2021	1958	−63	1.8	2.9	1.1	61
Sperry	1950	1966	16	1.3	1.3	0.0	0
Sperry	1960	1966	6	1.2	1.3	−0.1	0
Sperry	2014	1966	−48	0.8	1.3	−0.5	62

measurements and the geodetic balance. However, it ensures that both measurements reflect time-varying glacier area. It furthermore ensures geodetic mass balances accurately capture the long-term mass balance trend.

5. Conclusions

We quantified the bias introduced by fixed (maximum) glacier area handling in geodetic glacier mass balance. We described this bias in general terms and presented a means to correct the bias that can be applied to any glacier study where the maximum and minimum glacier areas during the measurement period are known, and the rate of glacier area change can be approximated as linear. However, we caution that the bias will be unpredictable if the fixed area treatment does not use the maximum glacier area. The bias scales with relative glacier area change and mass balance rate. Therefore, the fixed area bias is likely most problematic in regions where glaciers are retreating and thinning fast. This motivates improved glacier area data availability and clear reporting of the area-averaging treatment used in geodetic mass balance studies

Our analysis of five North American glaciers over various time intervals ranging from the mid-20th to early 21st century, showed that fixed (maximum) area handling consistently underestimates geodetic mass balance results by up to 19%, with the biggest discrepancy arising at South Cascade Glacier where large relative area changes are coupled with substantial elevation change.

Using fixed area treatment introduces a bias that systematically underestimates glacier mass balance. Whereas averaging across the maximum glacier area dampens the mass change signal, time-varying glacier area treatment yields geodetic balances that are comparable to glaciological and modeled conventional balances and translate to physical process insight.

If geodetic mass balance calculations do not account for glacier area change, then the m w.e. a^{-1} result cannot be compared across populations of glaciers with varying rates of area change. We suggest that geodetic mass balance calculations use time-evolving glacier area to reflect the dynamic glacier response to climate forcing whenever possible. In the absence of precise glacier area time series, studies will benefit from clear reporting of the glacier area treatment, to ensure inter-method comparisons are well understood.

References

Belart JMC and 5 others (2019) The geodetic mass balance of Eyjafjallajökull ice cap for 1945–2014: processing guidelines and relation to climate. *Journal of Glaciology* 65(251), 395–409. doi: 10.1017/jog.2019.16

Brun F, Berthier E, Wagnon P, Kääb A and Treichler D (2017) A spatially resolved estimate of High Mountain Asia glacier mass balances from 2000 to 2016. *Nature Geoscience* 10(9), 668–673. doi: 10.1038/ngeo2999

Cogley and 10 others (2011) *Glossary of mass balance and related terms.* IHP-VII Technical Documents in Hydrology No. 86, IACS Contribution No. 2, UNESCO-IHP, Paris.

Dussaillant BE and Brun F (2018) Geodetic mass balance of the Northern Patagonian Icefield from 2000 to 2012 using two independent methods. *Frontiers in Earth Science* 6(February), 1–13. doi: 10.3389/feart.2018.00008

Dussaillant I and 8 others (2019) Two decades of glacier mass loss along the Andes. *Nature Geoscience* 12(10), 802–808. doi: 10.1038/s41561-019-0432-5

Elsberg DH, Harrison WD, Echelmeyer KA and Krimmel RM (2001) Quantifying the effects of climate and surface change on glacier mass balance. *Journal of Glaciology* 47(159), 649–658. doi: 10.3189/172756501781831783

European Space Agency (2010) L1b NOP-IOP-GOP SAR, Version Baseline C.

European Space Agency (2022) Copernicus DEM. https://doi.org/10.5270/ESA-c5d3d65

Falaschi D and 6 others (2017) Mass changes of alpine glaciers at the eastern margin of the Northern and Southern Patagonian Icefields between 2000 and 2012. *Journal of Glaciology* 63(238), 258–272. doi: 10.1017/jog.2016.136

Falaschi D, Lenzano MG, Villalba R and Bolch T (2019) Six Decades (1958–2018) of Geodetic Glacier Mass Balance in Monte San Lorenzo, Patagonian Andes. 7(December). doi: 10.3389/feart.2019.00326

Farr TG and 17 others (2007) The Shuttle Radar Topography Mission. *Reviews of Geophysics* 45(2), 1–33. doi: 10.1029/2005RG000183.1.INTRODUCTION

Fischer M, Huss M and Hoelzle M (2015) Surface elevation and mass changes of all Swiss glaciers 1980–2010. *The Cryosphere* 9(2), 525–540. doi: 10.5194/tc-9-525-2015

Florentine C, Harper J, Fagre D, Moore J and Peitzsch E (2018) Local topography increasingly influences the mass balance of a retreating cirque glacier. *The Cryosphere* 12(6), 2109–2122. doi: 10.5194/tc-12-2109-2018

Hugonnet R and 10 others (2021) Accelerated global glacier mass loss in the early twenty-first century. *Nature* 592(7856), 726–731. doi: 10.1038/s41586-021-03436-z

Huss M (2013) Density assumptions for converting geodetic glacier volume change to mass change. *The Cryosphere* 7, 877–887.

Huss HR, Bauder A and Funk M (2012) Conventional versus reference-surface mass balance. *Journal of Glaciology* 58(208), 278–286. doi: 10.3189/2012JoG11J216

Jakob L, Gourmelen N, Ewart M and Plummer S (2021) Spatially and temporally resolved ice loss in High Mountain Asia and the Gulf of Alaska observed by CryoSat-2 swath altimetry between 2010 and 2019. *The Cryosphere* 15(4), 1845–1862. doi: 10.5194/tc-15-1845-2021

Kapitsa V, Shahgedanova M, Severskiy I and Kasatkin N (2020) Assessment of Changes in Mass Balance of the Tuyuksu Group of Glaciers, Northern Tien Shan, Between 1958 and 2016 Using Ground-Based Observations and Pléiades Satellite Imagery. *Frontiers of Earth Science.* doi: 10.3389/feart.2020.00259

Knuth F and 8 others (2023) Historical structure from motion (HSfM): automated processing of historical aerial photographs for long-term topographic change analysis. *Remote Sensing of Environment* 285(November 2022), 113379. doi: 10.1016/j.rse.2022.113379

Magnússon E, Belart JM, Pálsson F, Ágústsson H and Crochet P (2016) Geodetic mass balance record with rigorous uncertainty estimates deduced from aerial photographs and lidar data – Case study from Drangajökull ice cap, NW Iceland. *The Cryosphere* 10, 159–177. doi: 10.5194/tc-10-159-2016

McNabb R, Nuth C, Kääb A and Girod L (2019) Sensitivity of glacier volume change estimation to DEM void interpolation. *The Cryosphere* 13(3), 895–910. doi: 10.5194/tc-13-895-2019

McNeil C and 15 others (2019) Geodetic data for USGS benchmark glaciers: orthophotos, digital elevation models, glacier boundaries and surveyed positions (ver 3.0, August 2022). *U.S. Geological Survey data release.* https://doi.org/10.5066/P9R8BP3K

McNeil C and 6 others (2020) Explaining mass balance and retreat dichotomies at Taku and Lemon Creek Glaciers, Alaska. *Journal of Glaciology* 66(258), 530–532. doi: 10.1017/jog.2020.22

Menounos B and 11 others (2018) Heterogeneous changes in western North American glaciers linked to decadal variability in zonal wind strength. *Geophysical Research Letters* 46, 200–209. doi: 10.1029/2018GL080942

Mukherjee K, Menounos B, Shea JM and Mortezapour M (2022) Evaluation of surface mass-balance records using geodetic data and physically-based modelling, Place and Peyto glaciers, western Canada. *Journal of Glaciology* **276**, 665–682.

Neumann TA and 20 others (2019) The Ice, Cloud, and Land Elevation Satellite – 2 mission: A global geolocated photon product derived from the advanced topographic laser altimeter system. *Remote Sensing of Environment* **233**(November 2018), 111325. doi: 10.1016/j.rse.2019.111325

Nuth C and Kääb A (2011) Co-registration and bias corrections of satellite elevation data sets for quantifying glacier thickness change. *The Cryosphere* **5**(1), 271–290. doi: 10.5194/tc-5-271-2011

O'Neel S and 8 others (2019) Reanalysis of the US geological survey benchmark glaciers: long-term insight into climate forcing of glacier mass balance. *Journal of Glaciology* **65**(253), 850–866. doi: 10.1017/jog.2019.66

Paul F and 19 others (2013) On the accuracy of glacier outlines derived from remote-sensing data. *Annals of Glaciology* **54**(63), 171–182. doi: 10.3189/2013AoG63A296

Pfeffer WT and 75 others (2014) The Randolph Glacier Inventory: a globally complete inventory of glaciers. *Journal of Glaciology* **60**(221), 537–552. doi: 10.3189/2014JoG13J176

Porter C and 28 others (2018) ArcticDEM, Version 3. *Harvard Dataverse.* https://doi.org/10.7910/DVN/OHHUKH

Roberts-Pierel BM, Kirchner PB, Kilbride JB and Kennedy RE (2022) Changes over the last 35 years in Alaska's glaciated landscape: a novel deep learning approach to mapping glaciers at fine temporal granularity. *Remote Sensing* **14**(18), 4582. doi: 10.3390/rs14184582

Shean DE and 6 others (2016) An automated, open-source pipeline for mass production of digital elevation models (DEMs) from very-high-resolution commercial stereo satellite imagery. *ISPRS Journal of Photogrammetry and Remote Sensing* **116**, 101–117. doi: 10.1016/j.isprsjprs.2016.03.012

Shean DE and 5 others (2020) A systematic, regional assessment of High Mountain Asia Glacier Mass Balance. *Frontiers in Earth Science* **7**, 1–19. doi: 10.3389/feart.2019.00363

Sommer C and 5 others (2020) Rapid glacier retreat and downwasting throughout the European Alps in the early 21st century. *Nature Communications* **11**(1), 3209. doi: 10.1038/s41467-020-16818-0

U.S. ASTER Science Team (2022) ASTER Global Digital Elevation Model V003. *NASA EOSDIS Land Processes DAAC.* https://doi.org/10.5067/ASTER/ASTGTM.003

Vaughan D and 13 others (2013) *Climate Change 2013: The Physical Science Basis. Contribution of Working group I to the Fifth Assessment Report of the Intergovernmental Panel on Climate Change (IPCC).* Cambridge Univ. Press, Cambridge.

Wessel B and 5 others (2018) ISPRS journal of photogrammetry and remote sensing accuracy assessment of the global TanDEM-X digital elevation model with GPS data. *ISPRS Journal of Photogrammetry and Remote Sensing* **139**, 171–182. doi: 10.1016/j.isprsjprs.2018.02.017

Zemp M and 16 others (2013) Reanalysing glacier mass balance measurement series. *The Cryosphere* **7**(4), 1227–1245. doi: 10.5194/tc-7-1227-2013

Zemp M and 14 others (2019) Global glacier mass changes and their contributions to sea-level rise from 1961 to 2016. *Nature* **568**(7752), 382–386. doi: 10.1038/s41586-019-1071-0